*Thermochimica Acta*, 159 (1990) 55–66
Elsevier Science Publishers B.V., Amsterdam – Printed in The Netherlands


# THERMALLY INDUCED ISOMERIZATION AND DECOMPOSITION OF DIETHYLENETRIAMINE COMPLEXES OF ZINC(II) AND CADMIUM(II) IN THE SOLID STATE

SUBRATANATH KONER, ASHUTOSH GHOSH
and NIRMALENDU RAY CHAUDHURI *

*Department of Inorganic Chemistry, Indian Association for the Cultivation of Science, Jadavpur, Calcutta 700 032 (India)*

(Received 9 May 1989)

## ABSTRACT

Complexes of the form $[ML_2]X_2 \cdot nH_2O$ (where $M \equiv Zn^{II}$ or $Cd^{II}$, $L \equiv$ diethylenetriamine, and $n = 1$ when $X \equiv Cl^-$ or $Br^-$, $n = 3$ when $X \equiv 0.5SO_4^{2-}$ or $0.5SeO_4^{2-}$, $n = 0$ when $X = NO_3^-$ or $SCN^-$) have been synthesized, characterized and investigated thermally in the solid state. The complexes $[ZnL_2](SCN)_2$, $[CdL_2](SCN)_2$ and $[CdL_2](NO_3)_2$ undergo irreversible endothermic phase transitions. The complex $[ZnL_2]SeO_4 \cdot 3H_2O$ undergoes reversible endothermic phase transition after dehydration. The species [ZnLCl]Cl, $[CdLCl_2]$, $[ZnLSO_4]$, $[CdLSO_4]$ and $[ZnLSeO_4]$ have been synthesized pyrolytically in the solid state from their corresponding parent bis complexes and also from solution. The bis complexes have octahedral geometry, with the ligands arranged meridionally. The mono complexes of $Zn^{II}$ were found to have tetrahedral geometry, whereas those of $Cd^{II}$ seem to be octahedral.

## INTRODUCTION

Studies involving the synthesis and characterization of diethylenetriamine (L or dien) complexes of several metals are well documented in the literature [1–4], but thermal investigations of these complexes have not yet been carried out in the solid state. Recently, we reported novel thermally induced isomerization in the diethylenetriamine complexes of $Ni^{II}$ [5]. The present paper reports on thermal investigations of dien complexes of $Zn^{II}$ and $Cd^{II}$.

## EXPERIMENTAL

High purity diethylenetriamine was purchased from Koch–Light Lab. Ltd., and used as received. All the other chemicals used were of AR grade.

* Author to whom correspondence should be addressed.

0040-6031/90/$03.50 

TABLE 1

Analytical data for diethylenetriamine (L) complexes of Zn(II) and Cd(II)

| Compound | No. | Found (%) (Calc.) | | |
|---|---|---|---|---|
| | | Nitrogen | Carbon | Hydrogen |
| $[ZnL_2]Cl_2 \cdot H_2O$ | **1** | 23.2 | 26.5 | 7.9 |
| | | (23.3) | (26.6) | (7.8) |
| $[ZnL_2]Cl_2$ | **1a** | 24.7 | 28.5 | 8.0 |
| | | (24.5) | (28.0) | (7.6) |
| [ZnLCl]Cl | **1b** | 16.8 | 19.8 | 5.6 |
| | | (17.5) | (20.0) | (5.4) |
| $[ZnL_2]Br_2 \cdot H_2O$ | **2** | 18.9 | 21.3 | 6.4 |
| | | (18.7) | (21.3) | (6.2) |
| $[ZnL_2]Br_2$ | **2a** | 18.9 | 22.1 | 6.0 |
| | | (19.5) | (22.2) | (6.0) |
| [ZnLBr]Br | **2b** | 13.2 | 14.9 | 4.2 |
| | | (12.8) | (14.6) | (3.9) |
| $[ZnL_2]SO_4 \cdot 3H_2O$ | **3** | 19.7 | 23.0 | 7.7 |
| | | (19.7) | (22.7) | (7.6) |
| $[ZnL_2]SO_4$ | **3a** | 22.7 | 26.3 | 6.9 |
| | | (22.8) | (26.1) | (7.1) |
| $[ZnLSO_4]$ | **3b** | 15.6 | 18.3 | 5.1 |
| | | (15.9) | (18.1) | (4.9) |
| $[ZnL_2]SeO_4 \cdot 3H_2O$ | **4** | 17.8 | 20.1 | 7.1 |
| | | (17.9) | (20.5) | (6.8) |
| $[ZnL_2]SeO_4$ | **4a** | 20.3 | 23.5 | 6.7 |
| | | (20.3) | (23.1) | (6.3) |
| $[ZnLSeO_4]$ | **4c** | 13.6 | 15.3 | 4.1 |
| | | (13.5) | (15.4) | (4.2) |
| $[ZnL_2](SCN)_2$ [a] | **5** | 28.8 | 30.4 | 6.9 |
| | | (29.9) | (30.9) | (6.7) |
| $[ZnL_2](NO_3)_2$ | **6** | 28.4 | 24.5 | 6.3 |
| | | (28.3) | (24.3) | (6.6) |
| $[CdL_2]Cl_2 \cdot H_2O$ | **7** | 20.4 | 23.1 | 7.0 |
| | | (20.6) | (23.5) | (6.9) |
| $[CdL_2]Cl_2$ | **7a** | 21.5 | 24.5 | 6.5 |
| | | (21.6) | (24.6) | (6.7) |
| $[CdLCl_2]$ | **7b** | 14.8 | 17.0 | 4.8 |
| | | (14.7) | (16.8) | (4.5) |
| $[CdL_2]Br_2 \cdot H_2O$ | **8** | 16.7 | 19.2 | 5.6 |
| | | (16.9) | (19.3) | (5.6) |
| $[CdL_2]Br_2$ | **8a** | 17.1 | 19.9 | 5.6 |
| | | (17.5) | (20.0) | (5.4) |
| $[CdLBr_2]$ | **8b** | 11.5 | 12.9 | 3.6 |
| | | (11.2) | (12.8) | (3.5) |
| $[CdL_2]SO_4 \cdot 3H_2O$ | **9** | 17.5 | 20.4 | 6.4 |
| | | (17.9) | (20.5) | (6.8) |
| $[CdL_2]SO_4$ | **9a** | 20.1 | 23.2 | 6.5 |
| | | (20.2) | (23.1) | (6.3) |
| $CdLSO_4 \cdot H_2O$ | **9b** | 12.5 | 14.6 | 4.8 |
| | | (12.7) | (14.6) | (4.6) |

TABLE 1 (continued)

| Compound | No. | Found (%) (Calc.) | | |
|---|---|---|---|---|
| | | Nitrogen | Carbon | Hydrogen |
| $[CdLSO_4]$ | **9c** | 13.5 | 15.3 | 4.1 |
| | | (13.5) | (15.4) | (4.2) |
| $[CdL_2]SeO_4 \cdot 3H_2O$ | **10** | 16.3 | 18.4 | 6.1 |
| | | (16.3) | (18.6) | (6.2) |
| $[CdL_2]SeO_4$ | **10a** | 17.9 | 21.1 | 5.4 |
| | | (18.2) | (20.8) | (5.6) |
| $[CdL_2](SCN)_2$ [a] | **11** | 26.0 | 27.8 | 6.1 |
| | | (25.8) | (27.6) | (6.0) |
| $[CdL_2](NO_3)_2$ [a] | **12** | 25.7 | 21.7 | 5.9 |
| | | (25.3) | (21.7) | (5.9) |

[a] The analytical data for the post-phase species are similar to those for the pre-phase species.

The equipment employed for IR (ambient and above ambient), TG–DTA, DSC, X-ray powder diffraction and elemental analysis was as described in an earlier report [5]. Analytical, thermal, IR spectral and X-ray powder diffraction data are given in Tables 1, 2, 3 and 4, respectively.

*Preparation of the complexes*

$[ZnL_2]Cl_2 \cdot H_2O$ (**1**), $[ZnL_2]Br_2 \cdot H_2O$ (**2**), [ZnLCl]Cl (**1b**), [ZnLBr]Br (**2b**), $[CdLCl_2]$ (**7b**) and $[CdLBr_2]$ (**8b**) were prepared according to methods described in earlier reports [2,4].

$[ZnL_2](SCN)_2$ (**5**), $[ZnL_2](NO_3)_2$ (**6**) $[CdL_2]Cl_2 \cdot H_2O$ (**7**), $[CdL_2]Br_2 \cdot H_2O$ (**8**), $[CdL_2](SCN)_2$ (**11**) and $[CdL_2](NO_3)_2$ (**12**) were prepared by adding the ligand (L) (2–3) mmol) dropwise with constant stirring to the corresponding metal salt (1 mmol) in ethanolic medium. The complexes, which separated immediately, were filtered and washed with ethanol, and dried in a desiccator.

$[ZnL_2]SO_4 \cdot 3H_2O$ (**3**) and $[CdL_2]SO_4 \cdot 3H_2O$ (**9**) were prepared by adding the ligand (L) (2–3 mmol) dropwise to the correspondingly metal salt (1 mmol) dissolved in a minimum quantity of water (5 ml) with stirring. Ethanol was added with stirring until crystals separated, which were then filtered, washed with ethanol and dried.

$[ZnL_2]SeO_4 \cdot 3H_2O$ (**4**), $[CdL_2]SeO_4 \cdot 3H_2O$ (**10**), $[ZnLSO_4]$ (**3b**), $[ZnLSeO_4]$ (**4c**) and $CdLSO_4 \cdot H_2O$ (**9b**) were prepared according to the same procedure as in the case of (**3**), but using isopropanol in lieu of ethanol.

[ZnLCl]Cl (**1b**), $[ZnLSO_4]$ (**3b**), $[ZnLSeO_4]$ (**4c**), $[CdLCl_2]$ (**7b**) and $[CdLSO_4]$ (**9c**) were prepared thermally in the solid state by the temperature arrest technique from their respective parent bis complexes (Table 2).

TABLE 2

Thermal parameters for the Zn(II) and Cd(II) complexes of diethylenetriamine (L)

| Thermal reactions [a] | Temp. range (°C) | DTA peak temp. (°C) | |
|---|---|---|---|
| | | Endothermic | Exothermic |
| $[ZnL_2]Cl_2 \cdot H_2O$ (**1**) → $[ZnL_2]Cl_2$ (**1a**) | 130–163 | 146 | – |
| $[ZnL_2]Cl_2$ (**1a**) → [ZnLCl]Cl (**1b**) | 210–256 | 253 | – |
| [ZnLCl]Cl (**1b**) → $ZnCl_2$ | 260–380 | 264 [b] | 358 |
| $[ZnL_2]Br_2 \cdot H_2O$ (**2**) → $[ZnL_2]Br_2$ (**2a**) | 110–125 | 118 | – |
| $[ZnL_2]Br_2$ (**2a**) → [ZnLBr]Br (**2b**) | 230–318 | 271, 293 | – |
| [ZnLBr]Br (**2b**) → $ZnBr_2$ | 318–360 | 255, 275 | 355 |
| $[ZnL_2]SO_4 \cdot 3H_2O$ (**3**) → $[ZnL_2]SO_4$ (**3a**) | 59–110 | 105 | – |
| $[ZnL_2]SO_4$ (**3a**) → $[ZnLSO_4]$ (**3b**) | 180–242 | 240 | – |
| $[ZnLSO_4]$ (**3b**) → $ZnSO_4$ | 340–392 | 355 | 388 |
| $[ZnL_2]SeO_4 \cdot 3H_2O$ (**4**) → $[ZnL_2]SeO_4$ (**4a**) | 42–104 | 87 | – |
| $[ZnL_2]SeO_4$ (**4a**) → $[ZnL_2]SeO_4$ (**4b**) | 117.0–142.5 [c] | 123.0(sh), 134.4 [c] | – |
| $[ZnL_2]SeO_4$ (**4b**) → $[ZnL_2]SeO_4$ (**4a**) | 124.0–106.0 | – | 116.0 |
| $[ZnL_2]SeO_4$ (**4b**) → $[ZnLSeO_4]$ (**4c**) | 187–247 | 236 | – |
| $[ZnLSeO_4]$ (**4c**) → $ZnSeO_4$ | 267–289 | – | 282 |
| $[ZnL_2](SCN)_2$ (**5**) → $[ZnL_2](SCN)_2$ (**5a**) | 93.8–104.5 [c] | 100.1 [c] | – |
| $[ZnL_2](SCN)_2$ (**5a**) → (A) | 182–340 | 210 [b], 242 | 255 |
| $[ZnL_2](NO_3)_2$ (**6**) → (A) | 250–320 | 252 [b], 278 | 300 |
| $[CdL_2]Cl_2 \cdot H_2O$ (**7**) → $[CdL_2]Cl_2$ (**7a**) | 84–102 | 92 | – |
| $[CdL_2]Cl_2$ (**7a**) → $[CdLCl_2]$ (**7b**) | 185–230 | 221 | – |
| $[CdLCl_2]$ (**7b**) → $CdCl_2$ | 255–400 | 237 [b], 260 | 345, 350 |
| $[CdL_2]Br_2 \cdot H_2O$ (**8**) → $[CdL_2]Br_2$ (**8a**) | 80–112 | 89 | – |
| $[CdL_2]Br_2$ (**8a**) → $CdBr_2$ | 190–340 | 245, 260(sh) | – |
| $[CdL_2]SO_4 \cdot 3H_2O$ (**9**) → $[CdL_2]SO_4$ (**9a**) | 45–95 | 80 | – |
| $[CdL_2]SO_4$ (**9a**) → $[CdLSO_4]$ (**9c**) | 195–252 | 242 | – |
| $[CdLSO_4]$ (**9c**) → $CdSO_4$ | 278–335 | 325 | 330 |
| $CdLSO_4 \cdot H_2O$ (**9b**) → $[CdLSO_4]$ (**9c**) | 98–130 | 115 | – |
| $[CdLSO_4]$ (**9c**) → $CdSO_4$ | 290–370 | 325 | 335 |
| $[CdL_2]SeO_4 \cdot 3H_2O$ (**10**) → $[CdL_2]SeO_4$ (**10a**) | 50–101 | 89 | – |
| $[CdL_2]SeO_4$ (**10a**) → $CdSeO_4$ | 210–282 | 270 | 280 [d] |
| $[CdL_2](SCN)_2$ (**11**) → $[CdL_2](SCN)_2$ (**11a**) | 60.5–71.5 [c] | 65.4 [c] | – |
| $[CdL_2](SCN)_2$ (**11a**) → (A) | 175–305 | 190 [b] | 256 |
| $[CdL_2](NO_3)_2$ (**12**) → $[CdL_2](NO_3)_2$ (**12a**) | 122.5–140.0 [c] | 129.6 [c] | – |
| $[CdL_2](NO_3)_2$ (**12a**) → (A) | 265– [d] | – | 267 |

[a] (A) indicates that products have not been characterized.

[b] Peak due to melting.

[c] Temperatures taken from DSC curves.

[d] Sample swells here.

TABLE 3. IR spectral data (4000–400 $cm^{-1}$) for diethylenetriamine (L) complexes of zinc(II) and cadmium(II) in KBr

| Compound [a] | No. | Assignments [b] | | | | | | |
|---|---|---|---|---|---|---|---|---|
| | | $\nu(NH_2)$ | $\nu(CH_2)$ | $\delta(NH_2)$ | $\delta(CH_2)$ | $\rho_w(CH_2)+\rho_w(NH_2)+\tau(NH_2)+\tau(CH_2)$ + stretching vibrations of skeleton $\nu(C-N)+\nu(C-C)$ | $\rho_r(CH_2)$ | $\rho_r(CH_2)+\nu(MN)$ |
| $[ZnL_2](SCN)_2$ | **5** | 3320(sh), 3277(s), 3250(s), 3200(m), 3180(s) | 2940(s), 2910(s), 2880(s) | 1585(sbr) | 1490(s), 1470(s), 1445(sh), 1450(s) | 1385(s), 1365(m), 1322(s), 1325(m), 1305(m), 1290(m), 1255(s), 1148(s), 1120(w), 1110(vw), 1080(vs), 1035(s), 980(vsbr) | 910(m), 890(s), 870(vw), 830(w) | 602(s), 578(s), 530(w), 510(s), 500(s), 485(m), 572(m), 450(vw), 405(w), 385(w) |
| $[ZnL_2](SCN)_2$ | **5a** | 3320(sh), 3295(sbr), 3240(s), 3150(sh) | 2920(s), 2870(s) | 1570(s) | 1445(sbr) | 1380(w), 1350(s), 1322(s), 1320(s), 1300(w), 1285(m), 1255(s), 1145(m), 1120(w), 1070(vsbr), 1032(s), 1010(mbr), 950(sbr) | 910(w), 895(s), 870(w), 835(w) | 602(mbr), 560(s), 490(vsbr) |
| $[ZnL_2]SeO_4$ | **4a** | 3238(s), 3170(sbr), 3130(s) | 2930(sh), 2900(s), 2870(s) | 1580(s) | 1482(s), 1472(s), 1445(s) | 1385(s), 1360(ms), 1335(s), 1322(s), 1305(ms), 1280(m), 1251(s), 1150(m), 1140(w), 1070(sbr), 1025(mbr), 1001(s), 970(sbr) | [c] | 610(sh), 590(vsbr), 520(s), 490(ms), 401(sbr), 374(mbr) |
| $[ZnL_2]SeO_4$ | **4b** | 3235(s), 3185(sbr), 3135(s) | 2939(s), 2905(s), 2850(ms) | 1580(s) | 1451(sbr) | 1392(ms), 1465(w), 1345(sh), 1330(s), 1305(ms), 1290(sh), 1255(m), 1140(sbr), 1060(mbr) | [c] | 580(vsbr), 490(mbr), 385(mbr) |
| $[CdL_2](NO_3)_2$ | **12** | 3310(w), 3282(m), 3260(s), 3220(s), 3200(s), 3144(m) | 2940(m), 2910(m), 2880(s) | 1585(vsbr) | [c] | 1338(s), 1320(s), 1301(ms), 1278(w), 1262(m), 1245(vw), 1140(s), 1125(s), 1105(w), 1065(vs), 1038(ms), 1001(vs), 940(sbr) | 901(m), 882(vs), 865(w) | 601(sbr), 530(m), 505(s), 385(s), 330(mbr) |
| $[CdL_2](NO_3)_2$ | **12a** | 3307(w), 3300(w), 3258(s), 3210(mbr), 3140(m) | 3297(m), 2910(w), 2860(s) | 1590(mbr) | [c] | 1340(m), 1320(m), 1301(s), 1280(sh), 1260(w), 1245(w), 1140(m), 1125(m), 1065(s), 1035(s), 1000(s), 980(sh), 935(s), 920(sh) | 900(w), 880(s), 860(w) | 600(mbr), 525(w), 500(sbr), 425(w), 402(w), 380(m) |

[a] The IR spectra of the pre- and post-phase species of (11) are almost identical to those of (5) and (5a). [b] s = strong, m = medium, w = weak, v = very, br = broad, sh = shoulder. [c] Ligand bands are not distinguishable owing to overlapping with $SeO_4^{2-}$ and $NO_3^-$ bands.

TABLE 4

Prominent lines in the X-ray powder diffraction patterns of the pre- and post-phase species of complexes (**5**), (**11**) and (**12**)

| $d$ (Å) [a] | | | | | |
|---|---|---|---|---|---|
| $[ZnL_2](SCN)_2$ (**5**) | $[ZnL_2](SCN)_2$ (**5a**) [b] | $[CdL_2](SCN)_2$ (**11**) | $[CdL_2](SCN)_2$ (**11a**) [b] | $[CdL_2](NO_3)_2$ (**12**) | $[CdL_2](NO_3)_2$ (**12a**) [b] |
| 7.75(s) | 7.90(w) | 8.26(vs) | 9.01(w) | 7.89(sh) | 8.02(vs) |
| 7.31(s) | 7.52(vs) | 6.80(m) | 8.18(m) | 7.82(vs) | 7.89(s) |
| 6.75(vs) | 7.36(s) | 6.48(vs) | 7.46(vs) | 7.43(sh) | 6.50(m) |
| 6.32(s) | 6.61(s) | 6.14(s) | 6.50(vs) | 6.69(vs) | 6.12(w) |
| 5.86(w) | 6.32(w) | 5.46(w) | 5.55(m) | 6.50(s) | 5.71(w) |
| 5.09(s) | 5.90(s) | 5.08(w) | 4.92(m) | 5.57(m) | 5.21(s) |
| 4.46(vs) | 5.85(sh) | 4.34(vw) | 4.87(m) | 5.21(m) | 4.92(m) |
| 4.31(sh) | 4.82(vs) | 4.15(vw) | 4.67(w) | 4.55(m) | 4.66(sh) |
| 4.23(w) | 4.32(s) | 4.01(m) | 4.40(s) | 4.48(sh) | 4.65(m) |
| 3.96(w) | 4.12(w) | 3.95(sh) | 4.11(m) | 4.35(w) | 4.07(vs) |
| 3.86(w) | 4.01(m) | 3.64(m) | 3.95(w) | 4.26(vw) | 3.56(m) |
| 3.79(m) | 4.00(sh) | 3.56(w) | 3.81(vs) | 4.05(s) | 3.43(m) |
| 3.69(m) | 3.82(m) | 3.42(m) | 3.63(m) | 3.91(w) | 3.13(vs) |
| 3.63(m) | 3.76(s) | 3.38(s) | 3.55(m) | 3.81(w) | |
| 3.35(mbr) | 3.71(m) | 3.31(w) | 3.29(sh) | 3.54(m) | |
| 3.16(ms) | 3.65(s) | 3.06(w) | 3.25(s) | 3.42(m) | |
| 3.11(m) | 3.59(m) | | 3.11(w) | 3.09(vs) | |
| | 3.51(w) | | | 3.01(m) | |
| | 3.48(w) | | | | |

[a] v = very, s = strong, m = medium, w = weak, br = broad, sh = shoulder.

[b] Species **5a**, **11a** and **12a** were obtained after the phase transition of complexes **5**, **11** and **12**, respectively. The samples were cooled in a desiccator and X-ray powder patterns taken immediately thereafter.

## RESULTS AND DISCUSSION

### *Characterization of the complexes*

Recently, Searle and House [1] have used IR spectroscopy to characterize the three possible geometric isomers of $[CrL_2]^{3+}$, namely *u-fac*, *s-fac* and *mer*. Among these complexes, the *fac* isomers are characterized by a band at ca. 780 $cm^{-1}$, which is absent in the *mer* isomer. The spectrum of *u-fac* is very similar to that of *s-fac* in the region 950–750 $cm^{-1}$. However, the *u-fac* isomer can be distinguished by the presence of two bands in the region 1600–1500 $cm^{-1}$, whereas the *mer* and *s-fac* isomers have a single broad band at ca. 1570 $cm^{-1}$.

Among the bis-dien complexes considered here, the single crystal X-ray structures of $[ZnL_2]Br_2$ and $[ZnL_2](NO_3)_2$ have been described in the literature. In both cases the $[ZnL_2]^{2+}$ ion was found to exist in octahedral

geometry, with the ligands arranged meridionally [6,7]. The IR spectra of all the bis complexes of $Zn^{II}$ and $Cd^{II}$ considered in the present paper are exactly similar in the key regions 950–750 $cm^{-1}$ and 1600–1500 $cm^{-1}$, and are typical of the *mer* isomer. Therefore, it is concluded that all of these complexes possess *mer* octahedral geometry.

It is well known that the effect of size means that $Cd^{II}$ is more likely to assume a coordination number of six than is $Zn^{II}$ [8]. The far-IR spectrum of $[CdLCl_2]$ (**7b**) shows bands at 185 and 258 $cm^{-1}$ which are the characteristic bands of $\nu_b$(Cd–Cl) and $\nu_t$(Cd–Cl), respectively; and these bands are shifted to 158 and 186 $cm^{-1}$ in the case of $[CdLBr_2]$ (**8b**), in accordance with the literature value [9]. This observation indicates that the complexes $[CdLCl_2]$ (**7b**) and $[CdLBr_2]$ (**8b**) possess an octahedral geometry. Recently, Cannas and co-workers have shown by X-ray single crystal analysis that $[CdLCl_2]$ has a pseudo-octahedral chain structure [4]. By contrast, [ZnLCl]Cl (**1b**) shows two strong bands at 276 and 310 $cm^{-1}$, and these are shifted to 229 and 212 $cm^{-1}$ in the case of [ZnLBr]Br (**2b**). These two bands are the characteristic bands of $\nu_{as}$(Zn–X) and $\nu_s$(Zn–X) ($X \equiv Cl^-$ or $Br^-$), respectively, for pseudo-tetrahedral zinc complexes [9]. The complexes [ZnLCl]Cl (**1b**) and [ZnLBr]Br (**2b**) behave as 1 : 1 electrolytes in methanol ($\Lambda_m$ = 86 $\Omega^{-1}$ mol $cm^2$ and 92 $\Omega^{-1}$ mol $cm^2$ for **1b** and **2b**, respectively), which also indicates that one of the halide ions ($Cl^-$ or $Br^-$) should be coordinated to $Zn^{II}$. All these observations suggest a pseudo-tetrahedral structure for [ZnLCl]Cl (**1b**) and [ZnLBr]Br (**2b**). The other mono-dien complexes of $Zn^{II}$ and $Cd^{II}$, i.e. $[ZnLSO_4]$ (**3b**), $[ZnLSeO_4]$ (**4c**) and $[CdLSO_4]$ (**9c**), show IR spectra similar to those of their corresponding chloro or bromo analogues; but the actual coordination of $SO_4^{2-}$ or $SeO_4^{2-}$ is not explicable from the IR spectra, owing to the overlapping of amine bands.

*Thermal studies of the complexes*

*Irreversible phase transition of $[ZnL_2](SCN)_2$ (5), $[CdL_2](SCN)_2$ (11) and $[CdL_2](NO_3)_2$ (12)*

Upon heating, the complexes $[ZnL_2](SCN)_2$ (**5**), $[CdL_2](SCN)_2$ (**11**) and $[CdL_2](NO_3)_2$ (**12**) undergo irreversible endothermic phase transitions in the temperature ranges 93.8–104.5 °C ($\Delta H$ = 15.4 kJ $mol^{-1}$), 60.5–71.5 °C ($\Delta H$ = 12.6 kJ $mol^{-1}$) and 122.5–140.0 °C ($\Delta H$ = 15.4 kJ $mol^{-1}$), respectively (Fig. 1).

The IR spectra of the pre- and post-phase species were recorded (Table 3). For all the complexes, the spectral patterns in the regions 1600–1500 and 950–750 $cm^{-1}$ remain unchanged on phase transition, i.e. the IR spectra of both the pre- and post-phase species in these regions are characteristic of the *mer* isomer (see above). Thus, the possibility of geometrical isomerism can be discarded. However, the pre- and post-phase species of $[CdL_2](SCN)_2$ (**11**) and $[ZnL_2](SCN)_2$ (**5**) show some remarkable differences in the region

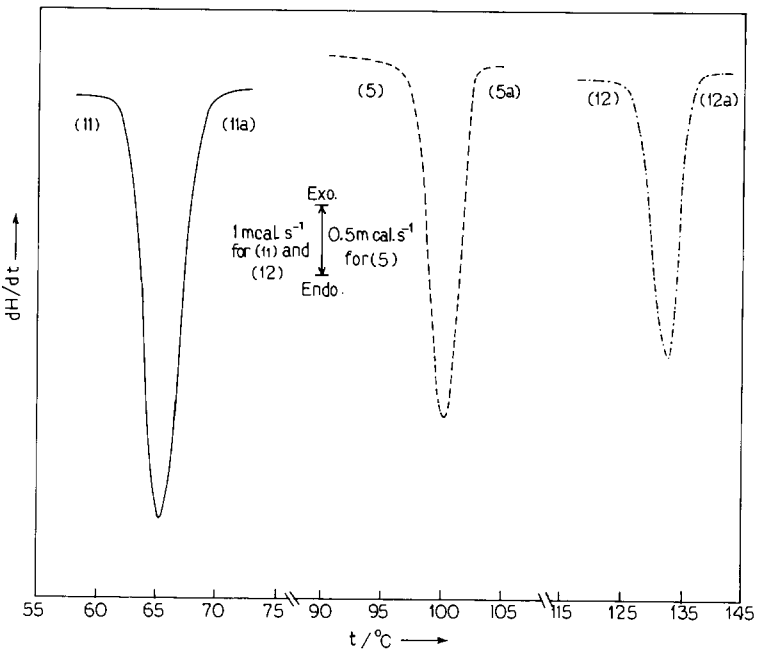


Fig. 1. DSC curves for: $[CdL_2](SCN)_2$ (**11**), sample mass = 9.92 mg (———); $[ZnL_2](SCN)_2$ (**5**), sample mass = 9.37 mg (– – –); and $[CdL_2](NO_3)_2$ (12), sample mass = 8.83 mg (– · – · –).

1500–1400 $cm^{-1}$, where $\delta(CH_2)$ vibration occurs. In contrast to the three distinct strong bands at ca. 1490, 1470 and 1450 $cm^{-1}$ for complexes **5** and **11**, the corresponding post-phase species show only one broad band at ca. 1450 $cm^{-1}$ (Table 3). Besides this, overall broadening and some changes of band positions and intensity ratios in the $\nu(NH_2)$ and $\nu(CH_2)$ regions were also observed. In the case of $[CdL_2](NO_3)_2$ (**12**), the change in $\delta(CH_2)$ bands was not clearly seen, owing to the overlapping of $NO_3^-$ bands, but broadening and shifting of other band positions was observed. We have noted in previous works that conformational isomers of the diamine [10–12] and triamine [5] systems show similar types of differences in their IR spectra. As a consequence, conformational changes of the triamine chelate rings are assumed to be responsible for the phase transitions. The X-ray powder diffraction patterns of post-phase species of complexes **5**, **11** and **12** (Table 4) differ significantly from their corresponding parent complexes, suggesting that a substantial change in the unit cell shape occurs during the phase transition. These differences between the X-ray powder diffraction patterns of the pre- and post-phase species are not inconsistent with the conformational changes observed previously [5,10–12]. It may be noted here that the complex $[ZnL_2](NO_3)_2$ (**6**) does not show any phase transition before decomposition (Table 2).

It is interesting to note that on being kept in a humid atmosphere (relative humidity 70–80%), the post-phase species revert to their corresponding

pre-phase form, but that they can retain their identity in a desiccator. This reversal also takes place if the post-phase species are suspended in any solvent, e.g. methanol, ethanol, acetonitrile, etc. We have noted this type of reversion before, and have proposed a plausible mechanism [10,11]. A similar mechanism seems to be operative for the reversions reported in the present work.

*Reversible phase transition of* $[ZnL_2]SeO_4 \cdot 3H_2O$ *(4)*

On heating, the complex $[ZnL_2]SeO_4 \cdot 3H_2O$ (**4**) becomes anhydrous **4a** at 104°C (Figs. 2 and 3). On further heating, this anhydrous form **4a** undergoes a reversible phase transition (117.0–142.5°C; $\Delta H = 3.4$ kJ mol$^{-1}$) with two overlapping endotherms (peak temp. = 123.0 and 134.4°C), transforming into its isomer **4b**. On cooling, this isomer (**4b**) reverts to its original anhydrous form **4a** showing only one exotherm (124.0–106.0°C; $\Delta H = 2.1$ kJ mol$^{-1}$; peak temp. = 116.0°C) (Fig. 2, Table 2). On recycling, the temperature range as well as the nature of the DSC curves of successive heating and cooling remain the same.

The characteristic band of the *mer* isomer in the region 950–750 cm$^{-1}$ could not be identified, owing to overlapping of the $\nu_3$ band of $SeO_4^{2-}$ in **4**, **4a** and **4b**, but the remaining part of the IR spectra of each of these complexes is similar to that of the other *mer* isomer. It can therefore be assumed that species **4**, **4a** and **4b** are octahedral, with the ligands arranged meridionally.

Comparison of the IR spectra of **4a** and **4b** shows the same differences as observed for the pre- and post-phase species of **5** and **11**. Therefore, in this case also, similar types of conformational changes of the chelate rings are

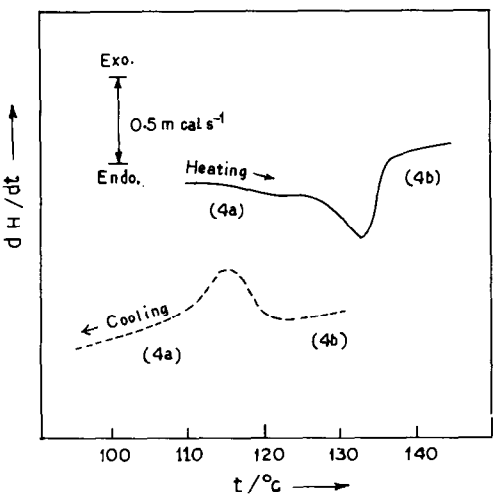


Fig. 2. DSC curves for $[ZnL_2]SeO_4$ (**4a**), sample mass = 12.68 mg: heating (———) and cooling (– – –).

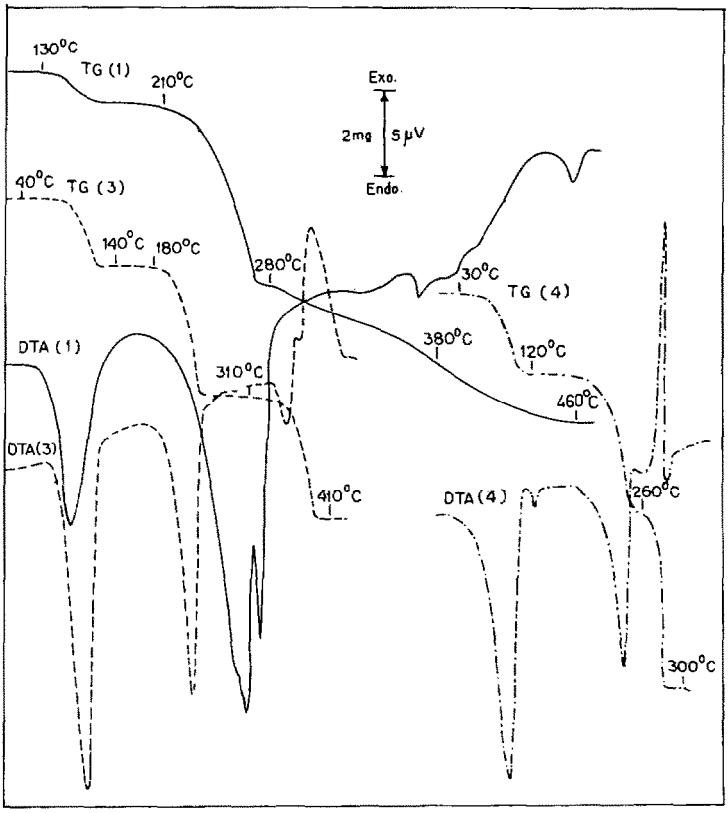


Fig. 3. Thermal curves for: $[ZnL_2]Cl_2 \cdot H_2O$ (**1**), sample mass = 13.22 mg (———); $[ZnL_2]SO_4 \cdot 3H_2O$ (**3**), sample mass = 12.55 mg (– – –); and $[ZnL_2]SeO_4 \cdot 3H_2O$ (**4**), sample mass = 14.63 mg (– · – · –).

probably associated with the phase transition. The X-ray powder diffraction patterns of **4a** and **4b** could not be determined, owing to the extreme hygroscopic nature of the species, and the lack of a high-temperature X-ray facility, respectively.

It is interesting to note that the energy requirement (Table 2) for the phase transition of $[ZnL_2]SeO_4 \cdot 3H_2O$ (**4**) is much lower than for complexes **5**, **11** and **12**. This lower value can probably be explained as follows. During the dehydration of complex **4** it is likely that a considerable number of vacant sites are created in the crystal lattice. This would increase the flexibility of the triamine chelate rings, and hence their susceptibility to conformational change. Naturally, the energy requirement for phase transition would then be lower.

*Decomposition of the complexes*

The decomposition of complexes **1**, **2**, **3**, **4**, **7** and **9** is interesting as the process involves the formation of the mono complex as an isolable inter-

mediate. (The species [ZnLBr]Br (**2b**) could not be isolated in a pure form during the thermal decomposition of **2a**, although the TG curve does show a break for the formation of [ZnLBr]Br.) All the mono species were also synthesized from solution. The thermal and IR spectral behaviours of the mono species synthesized from solution are almost identical to those of the mono species synthesized pyrolytically, except in the case of **8b**, which was obtained as a hydrated complex from solution (Table 2). Complexes **8** and **10** decompose directly to the corresponding metal salt without showing any break in their TG curves, while complexes **5**, **6**, **11** and **12** decompose via a complicated reaction path. The end products were not characterized for these complexes (Table 2).

The decomposition processes of complexes **1**, **2**, **3**, **4**, 7 and **9** are discussed below in more detail.

Upon heating, $[ZnL_2]Cl_2 \cdot H_2O$ (**1**) becomes dehydrated at 163°C and transforms to $ZnCl_2$ at 380°C via [ZnLCl]Cl (**1b**) at 260°C. $[ZnL_2]SO_4 \cdot 3H_2O$ starts to lose water molecules at 59°C and becomes completely dehydrated at 110°C. On further heating, $[ZnL_2]SO_4$ (**3a**) transforms to $ZnSO_4$ at 392°C via $[ZnLSO_4]$ (**3b**) at 242°C. $[ZnL_2]SeO_4$ (**4b**) transforms to the metal salt at 289°C via the isolable intermediate $[ZnLSeO_4]$ (**4c**) at 247°C (Fig. 3). $[CdL_2]Cl_2 \cdot H_2O$ (7) becomes dehydrated at 102°C. On further heating, the species (**7a**) decomposes to $CdCl_2$ at 400°C via $[CdLCl_2]$ (**7b**) at 230°C. $[CdL_2]SO_4 \cdot 3H_2O$ (**9**) becomes dehydrated at 95°C and

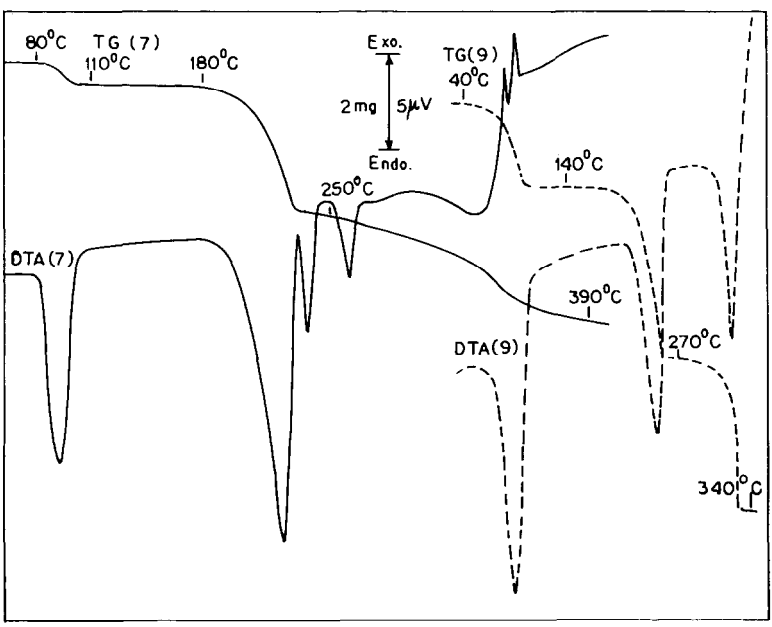


Fig. 4. Thermal curves for: $[CdL_2]Cl_2 \cdot H_2O$ (7), sample mass = 9.97 mg (———); and $[CdL_2]SO_4 \cdot 3H_2O$ (**9**), sample mass = 15.62 mg (– – –).

transforms to $CdSO_4$ at 335 °C via the isolable intermediate [$CdLSO_4$] (**9c**) at 252 °C (Fig. 4). On crystallization from a water–isopropanol mixture (9 : 1), the pyrolytically isolated species [$CdLSO_4$] (**9c**) yields $CdLSO_4 \cdot H_2O$ (**9b**) which is exactly similar to complex **9b** as prepared from solution.

ACKNOWLEDGEMENT

We are grateful to the Department of Geological Sciences, Jadavpur University, Calcutta 700 032 for X-ray powder diffraction analyses.

REFERENCES

1 G.H. Searle and D.A. House, Aust. J. Chem., 40 (1987) 361; and references therein.
2 N.F. Curtis and H.K.J. Powell, J. Chem. Soc. A, (1968) 3069.
3 D.N. Hague and A.D. Moreton, J. Chem. Soc., Dalton Trans., (1987) 2889; and references therein.
4 M. Cannas, G. Marongiu and G. Saba, J. Chem. Soc., Dalton Trans., (1980) 2090.
5 S. Koner, A. Ghosh and N. Ray Chaudhuri, Transition Met. Chem., 13 (1988) 291.
6 P.G. Hodgson and B.R. Penfold, J. Chem. Soc., Dalton Trans., (1974) 1870.
7 M. Zocchi, A. Albinati and G. Tieghi, Cryst. Struct. Commun., 1 (1972) 135.
8 F.A. Cotton and W. Wilkinson, Advanced Inorganic Chemistry, Wiley, New York, 4th ed., 1980, p. 590.
9 F. Cariati, G. Ciani, L. Menabue, G.C. Pellacani, G. Rassu and A. Sironi, Inorg. Chem., 22 (1983) 1897.
10 G. De, P.K. Biswas and N. Ray Chaudhuri, J. Chem. Soc., Dalton Trans., (1984) 2591.
11 A. Ghosh, G. De and N. Ray Chaudhuri, J. Chem. Res., (1987) 105.
12 A.K. Mukherjee, M. Mukherjee, A.J. Welch, A. Ghosh, G. De and N. Ray Chaudhuri, J. Chem., Soc., Dalton Trans., (1987) 997.